

NUMERICAL INVESTIGATION OF STRUCTURE-BORNE INTERIOR NOISE IN FLEXIBLE RECTANGULAR BOXES

VB Georgiev Department of Aeronautical and Automotive Engineering,
VV Krylov Loughborough University
Loughborough, Leicestershire LE11 3TU, UK

1 INTRODUCTION

Flexible rectangular box structures, often called box-like structures, are used widely in a large number of engineering applications, e.g. as elements of railway carriages, heavy goods vehicles, buildings, civil-engineering constructions, etc. Although all-flexible rectangular boxes represent one of the geometrically simple types of engineering structures, the analysis of their structural-acoustic properties is rather difficult, and it can not be performed in terms of closed form solutions. Apparently, the first work in this area has been published by Dickinson and Warburton¹ who have obtained approximate analytical expressions for natural frequencies of uncoupled vibrations of all-flexible box structures. These authors also performed experimental measurements of the natural frequencies for a box structure. Later, Hooker and O'Brien² have calculated first natural frequencies for a box of the same dimensions using finite element (FE) method and compared them with the approximate analytical and experimental results of Dickinson and Warburton¹. More recently, authors of Reference 3 used FE calculations to carry out vibration analysis of a thin-plate box, considering only in-plane motion. Later on they extended their study, analyzing flexural vibrations of the same model using a combination of FE and analytical approaches⁴. Vibrations of rectangular box-like structures have been also investigated analytically using some simple approximations, e.g. taking into account only in-plane waves transmitted to the adjacent walls under the impact of the initially flexural waves^{5,6}. Some authors utilized rectangular box models to verify different optimization procedures for noise reduction⁷⁻¹⁰.

In spite of the extensive use of the above-mentioned all-flexible rectangular box structures, their coupled structural-acoustic behavior was not analyzed. The aim of this paper is to carry out a comprehensive numerical investigation of structural-acoustic properties of all-flexible rectangular boxes. In the first part of the paper, the attention will be paid to understanding the uncoupled structural and acoustic properties of flexible rectangular boxes. This part largely re-visits the results obtained in the pioneering papers^{1,2}. A comparison will be made, where possible, of the results obtained in the present paper with the results of References 1,2. In the second part of the paper, the coupled structural-acoustic properties of all-flexible rectangular boxes will be studied.

2 STRUCTURAL AND ACOUSTIC ANALYSIS OF THE UNCOUPLED MODEL

The basic model under consideration represents an all-flexible rectangular box made of steel (with the values of Young's modulus $E = 2 \cdot 10^{11}$ N/m², Poisson ratio $\sigma = 0.31$ and mass density $\rho = 7950$ kg/m³), and all the walls of the box structure have the same thickness. The only boundary conditions imposed on the model are applied at the corners of the bottom plate, which simulates fixing the box at four points to a rigid foundation. The model dimensions are as follows: $x = 2.4$ m (length), $y = 1.4$ m (height) and $z = 1.5$ m (width). The wall thickness of the model was chosen to be 8 mm, which corresponds to a fundamental structural vibration frequency of about 15–20 Hz.

Using finite element software, MSC.Nastran and MSC.Patran, the uncoupled normal vibration modes and the corresponding natural frequencies of the all-flexible box structure under consideration have been analyzed. Note that 'free' boundary conditions were adopted everywhere in the uncoupled analysis, whereas in the coupled analysis the model was considered as being placed on a certain foundation. In other words, the boundary conditions utilized in the coupled analysis simulated an attaching mechanism, which restricts the structural behavior of the model. In the uncoupled analysis, a refined finite element mesh was used consisting of 7248 CQUAD finite elements - for the structural sub-system, and 5040 CHEXA finite elements - for the acoustic sub-system.

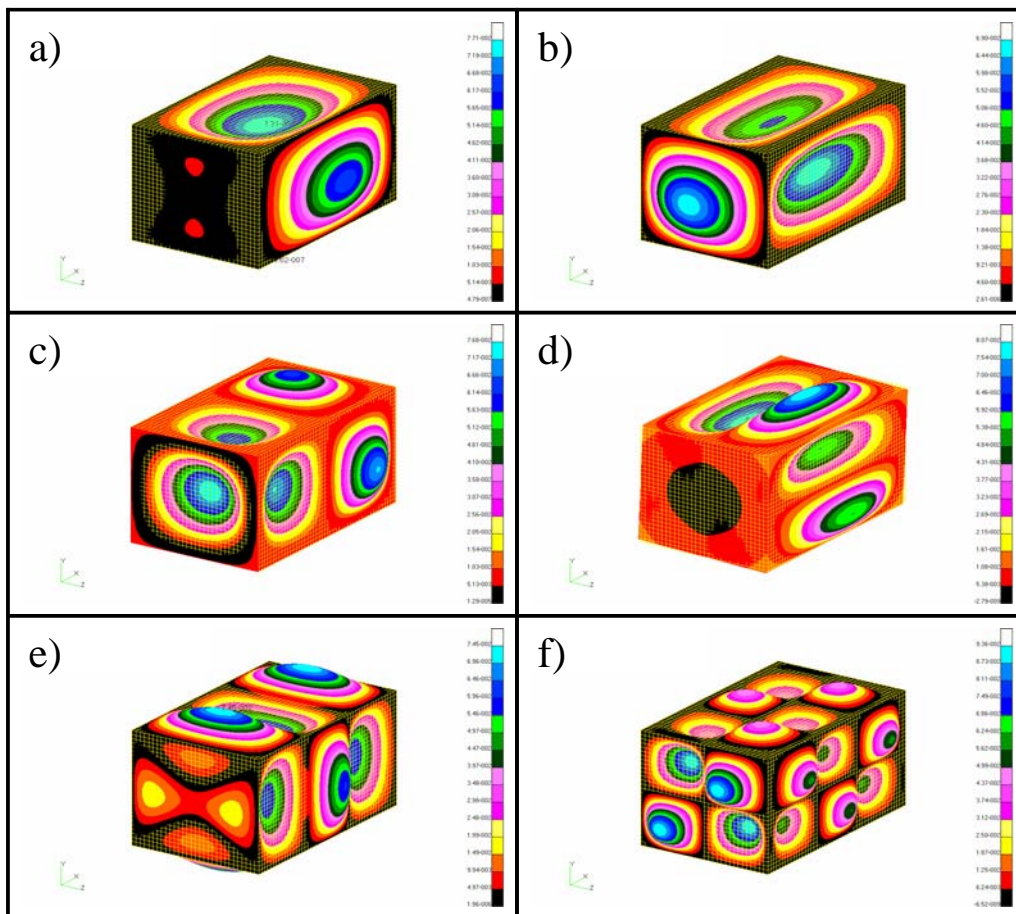


Figure 1. Some structural modes of a rectangular box, at: a) 13.692 Hz, b) 22.069 Hz, c) 34.730 Hz, d) 42.138 Hz, e) 43.541 Hz and f) 90.904 Hz.

Figure 1 shows some structural vibration modes calculated for the uncoupled rectangular box model. As the box structure under consideration is fully symmetrical in respect of the three orthogonal coordinate planes, a number of symmetric and anti-symmetric structural modes occur (see also Reference 2). In the 3-D picture (Fig. 1), the symmetric and anti-symmetric normal modes can not be seen clearly. This is why in Figure 2 the same normal modes are presented in XY (vertical) plane, where symmetric and anti-symmetric modes are clearly seen.

Note that, in addition to the existence of symmetric and anti-symmetric modes, all-flexible rectangular box structures exhibit another interesting phenomenon well known from the general

symmetry considerations, namely the presence of repeated frequencies associated with degenerate modes. This phenomenon occurs in rectangular boxes of higher symmetry. To illustrate it numerically, some additional calculations (not shown here for brevity) have been conducted in the present work for a cubic box model with the dimensions (1, 1, 1) m and for a rectangular box model with the dimensions (2.4, 1.5, 1.5) m respectively along the coordinates x, y and z.

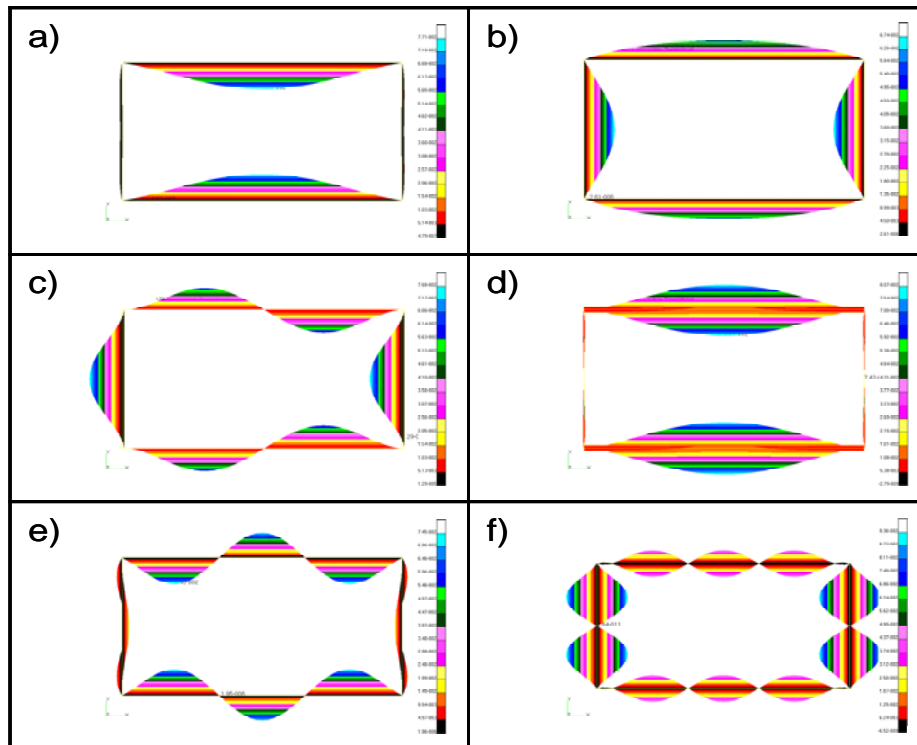


Figure 2. Symmetric and anti-symmetric normal modes at: a) 13.692 Hz, b) 22.069 Hz, c) 34.730 Hz, d) 42.138 Hz, e) 43.541 Hz and f) 90.904 Hz.

In Table 1, Columns 3, 4 and 5, the first ten analytically calculated natural frequencies of the separate plate components satisfying simply supported boundary conditions are presented. One can see that resonant frequencies of these plates are noticeably different from the **FE** results for the resonant frequencies of the full box structure (columns 1 and 2 in Table 1). This reflects the lack of the possibility to approximate rectangular box resonant frequencies by resonant frequencies of its separate plate components.

Note that the natural frequencies of the full box structure presented in Table 1 have been calculated for the two cases: with 'free' boundary conditions (column 1) and with simply supported boundary conditions imposed on the all edges of the model (column 2). Despite some discrepancies between these sets of frequencies, their closeness, at least for the first eight modes, is indicative. In this frequency range, the structure under both sets of boundary conditions has high modal density. This is why under 'free' boundary conditions there are 312 resonance peaks in this range (excluding the first six rigid-body natural frequencies) and the last one occurs at 498.90 Hz, whereas under simply supported boundary conditions the result is 311 peaks with the last natural frequency at 499.99 Hz.

№	Box structure, natural frequencies, Hz		Plate component 1, natural frequencies, Hz	Plate component 2, natural frequencies, Hz	Plate component 3, natural frequencies, Hz	Acoustic, FE calculated, natural frequencies, Hz	Acoustic, exact, natural frequencies, Hz
	1	2	3	4	5	6	7
1	13.692	13.693	11.805 (1, 1)	13.061 (1, 1)	18.209 (1, 1)	69.07 (1, 0, 0)	69.02 (1, 0, 0)
2	19.306	17.019	21.726 (2, 1)	22.974 (2, 1)	43.609 (2, 1)	110.6 (0, 0, 1)	110.4 (0, 0, 1)
3	20.749	18.506	37.282 (1, 2)	39.514 (3, 1)	47.387 (1, 2)	118.5 (0, 1, 0)	118.3 (0, 1, 0)
4	22.069	22.074	38.275 (3, 1)	42.307 (1, 2)	72.463 (2, 2)	130.4 (1, 0, 1)	130.2 (1, 0, 1)
5	24.821	23.834	47.090 (2, 2)	52.094 (2, 2)	85.958 (3, 1)	137.2 (1, 1, 0)	137.0 (1, 1, 0)
6	26.290	25.876	61.448 (4, 1)	62.675 (4, 1)	96.024 (1, 3)	138.4 (2, 0, 0)	138.0 (2, 0, 0)
7	28.509	26.652	63.458 (3, 2)	68.427 (3, 2)	114.33 (3, 2)	162.2 (0, 1, 1)	161.9 (0, 1, 1)
8	29.983	27.250	79.735 (1, 3)	91.038 (1, 3)	120.62 (2, 3)	176.2 (1, 1, 1)	175.9 (1, 1, 1)
9	34.730	28.773	86.394 (4, 2)	91.317 (4, 2)	145.23 (4, 1)	177.2 (2, 0, 1)	176.8 (2, 0, 1)
10	42.138	34.276	89.381 (2, 3)	92.450 (5, 1)	161.70 (3, 3)	182.2 (2, 1, 0)	181.8 (2, 1, 0)

Table 1. Structural and acoustic natural frequencies of an uncoupled box model.

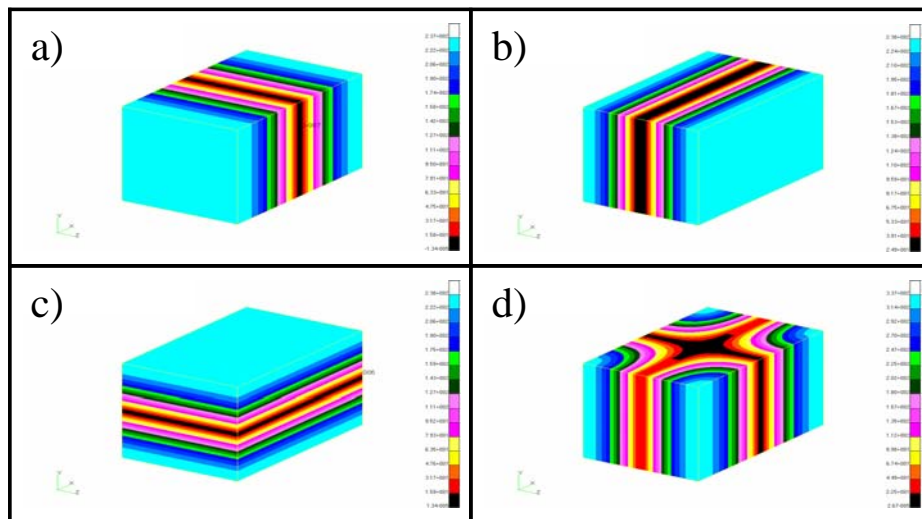


Figure 3. First four uncoupled acoustic modes of a rectangular box enclosure, at: a) 69.07 Hz, b) 110.64 Hz, c) 118.57 Hz and d) 130.43 Hz.

Figure 3 and Table 1 show some of the normal modes and natural frequencies of the uncoupled acoustic sub-system. The comparison between the analytically calculated natural frequencies (Table 1, Column 7), which are determined very easily for the acoustic rectangular sub-system, and those calculated using finite element techniques (Table 1, Column 6) shows a good agreement between them and thus validates the chosen mesh size.

It is interesting to compare the results of the present numerical approach with the results obtained experimentally and theoretically by the earlier authors. For that purpose, a box structure with the dimensions $x = 0.36576$, $y = 0.3048$ and $z = 0.24384$, m has been calculated, i.e. the same one that has been used by Dickinson and Warburton [1] and by Hooker and O'Brien [2].

№	Theoretical frequencies, Hz, (Dickinson and Warburton 1967)	Experimental frequencies, Hz, (Dickinson and Warburton 1967)	FE frequencies, Hz, (Present work)	FE frequencies, Hz, (Hooker and O'Brien 1974)
1	2	3	4	5
1	179	178	178.53	184
2	203	228	230.36	206
3	258	264	270.88	262
4	272	282	281.87	279
5	283	297	301.85	291
6	333	328	331.54	336
7	384	395	397.82	394
8	397	399	399.16	409
9	437	451	449.87	452
10	455	479	473.91	465
11	486	495	485.43	497
12	499	497	499.29	512
13	570	571	565.08	588
14	577	580	575.10	595
15	624	634	625.15	669
16	648	642	640.51	671

Table 2. Measured and calculated natural frequencies of vibration for Dickinson and Warburton's box model.

In Table 2, the natural frequencies of the model under consideration obtained by different authors are presented. The approximate analytical results of Dickinson and Warburton¹ are shown in Column 2, whereas Column 3 presents their experimental results. In Column 4, the numerical results of the present paper are shown. In Column 5, a set of numerical data obtained by Hooker and O'Brien² can be seen. As one can see, there is a good agreement between the experimental measurements (Column 3) and the numerical results of the present paper (Column 4). Comparing the **FE** results of the present work and of the work of Hooker and O'Brien² with the experimental results, one can see a noticeable improvement in accuracy of numerically calculated natural frequencies in the present paper as compared to those calculated by Hooker and O'Brien². Comparing the present **FE** results with the approximate analytical calculations of Dickinson and Warburton¹, one can see that the precision of the latter is generally not as good as that of the present work, but it is better than the precision achieved by Hooker and O'Brien².

3 STRUCTURAL-ACOUSTIC ANALYSIS OF THE FULLY COUPLED MODEL

In this section, fully coupled structural-acoustic modes are investigated, and a set of structural-acoustic frequency response functions (**FRF's**) at specific acoustic nodes are discussed and compared. As was mentioned above, simply supported boundary conditions at the corner nodes of the bottom plate were imposed to simulate an attaching mechanism. In the coupled model, 1812 CQUAD structural finite elements and 5040 CHEXA acoustic finite elements were used. Energy losses in the structure were modeled using 3 % damping factor. As far as air acoustic losses are concerned, a simple damping coefficient of 1 % was used for the sake of simplicity.

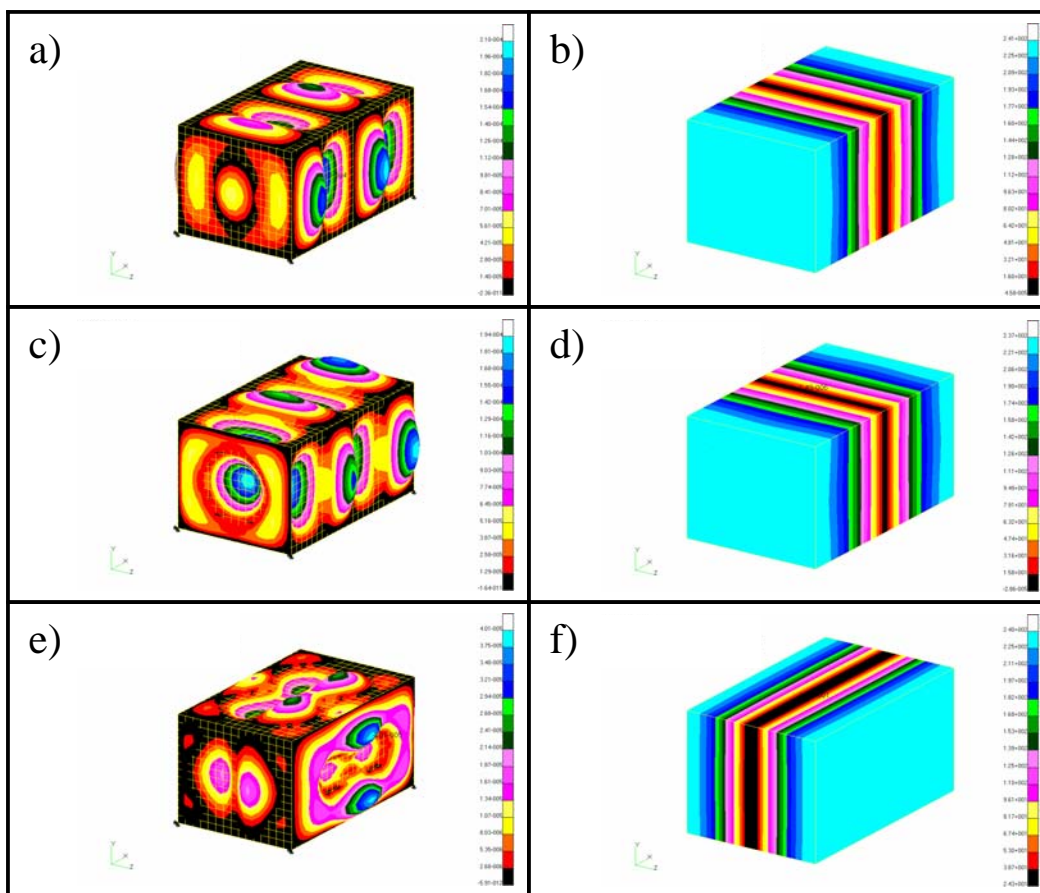


Figure 4. Normal modes of a coupled box model: a,b) at 68.352 Hz; c,d) at 71.848 Hz; and e, f) at 111.72 Hz.

In Figure 4, some of the normal modes of the fully coupled model, that are influenced by the first and second uncoupled acoustic modes, are presented. As it is well known¹¹, the coupling depends on the spatial similarity and frequency closeness between the uncoupled structural and acoustic normal modes. Therefore, some of the structural modes can couple better with certain acoustic mode, in contrast to others. The three normal modes shown in Figure 4, at about 68, 71 and 111 Hz, are not much affected by the coupling effects and are very similar to the corresponding uncoupled modes.

In Figure 5, the structural-acoustic pressure **FRF**'s calculated in the center of the box interior (at node 4826) are shown for the driving force with the amplitude of 200 N applied in the center and in the vicinity of a corner of the bottom plate. In Figure 6, the **FRF**'s are plotted at node 4826 (at the centre of the box) and at node 6825 (away from the centre) for a driving force applied close to a corner of the bottom plate.

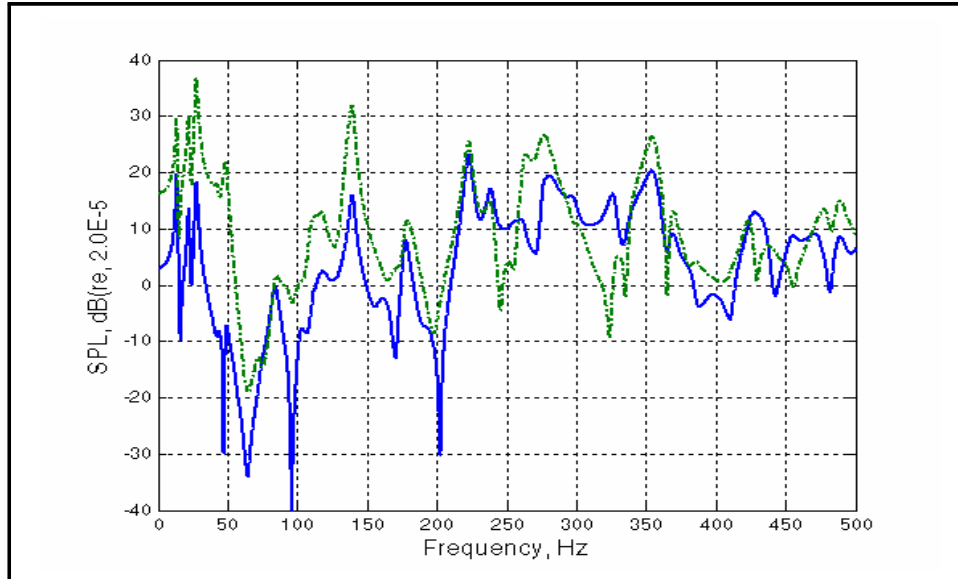


Figure 5. Structural-acoustic FRF's calculated at node 4826 for a driving force applied close to a corner (solid curve) and in the centre of the bottom plate (dash-dotted curve).

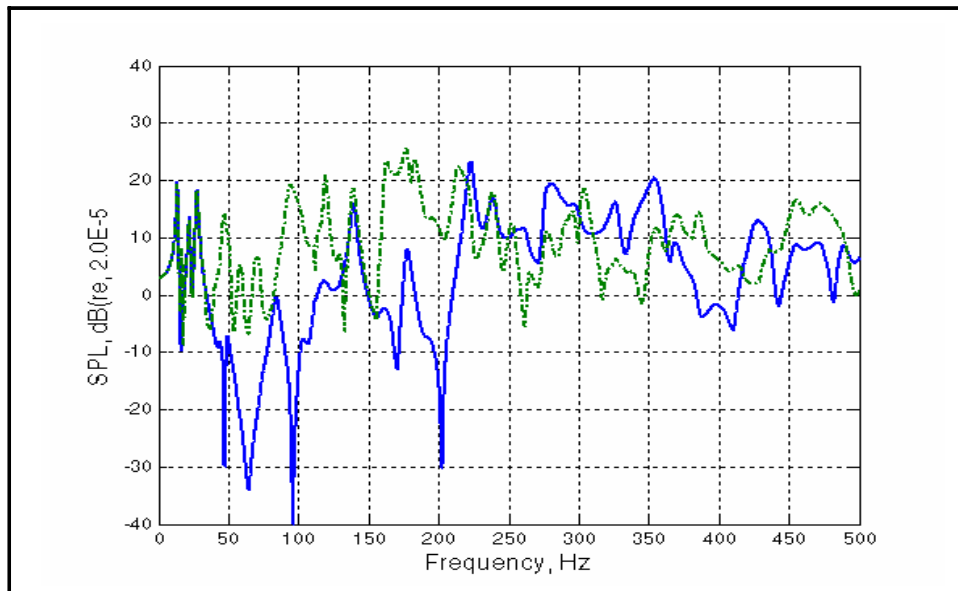


Figure 6. Structural-acoustic FRF's calculated at node 4826 (solid curve) and at node 6825 (dash-dotted curve) for a driving force applied close to a corner of the bottom plate.

Taking into account the value of the first uncoupled acoustic natural frequency of the model, which is about 69 Hz, the graphs presented in Figures 5 and 6 can be regarded as consisting of two parts. The first part, below 69 Hz, represents the area where **FRF's** are induced by structural vibrations of the model defined by the location of the driving force. The second part, above 69 Hz, is the area where **FRF's** are formed by a complex interaction of the structural and fluid vibrations. In this area, above 69 Hz in Figures 5 and 6, the **FRF's** demonstrate more complex behaviour depending on the positions of both the driving force and the receiver. If a driving force acts close to a nodal line of a structural model, then the force can not excite many of the structural normal modes and the pressure response inside the model will be much lower in a certain frequency range. In practice, a complex geometry of the structure and a high density of the normal modes make it quite difficult to find the appropriate nodal lines. However, in the case of success, a noticeable noise reduction can be achieved.

4 CONCLUSIONS

A comprehensive finite element analysis of structural, acoustic, and coupled structural-acoustic properties of all-flexible rectangular boxes has been carried out. The initial attention has been paid to the uncoupled structural behaviour of the model, where the results of the pioneering papers^{1,2} have been revisited and their accuracy improved. In the second part of the paper, a fully coupled structural-acoustic analysis has been undertaken for the first time. A number of coupled structural-acoustic modes and a set of structural-acoustic frequency response functions have been calculated and analysed for different positions of a driving force and a receiver.

5 REFERENCES

1. S.M. Dickinson and G.B. Warburton, Vibration of box-type structures, *Journ. Mech. Eng. Sci.*, 9, 325-334 (1967).
2. R.J. Hooker and D.J. O'Brien, Natural frequencies of box-type structures by a finite element method, *Journal of Applied Mechanics*, 41, 363-365 (1974).
3. R.M. Grice and R.J. Pinnigton, . Vibration analysis of a thin-plate box using a finite element model which accommodates only in-plane motion, *Journal of Sound and Vibration*, 232, 449-471 (2000).
4. R.M. Grice and R.J. Pinnigton, Analysis of the flexural vibration of a thin-plate box using a combination of finite element analysis and analytical impedances, *Journal of Sound and Vibration*, 249, 499-527 (2002).
5. R.A. Fulford and B.A.T. Petersson, Estimation of vibrational power in built-up systems involving box-like structures, part 1: Uniform force distribution, *Journal of Sound and Vibration*, 232, 877-895 (2000).
6. B.A.T. Petersson, Vibro-acoustic features of box-like structures, *Proceedings of NOVEN 2005*, Saint Raphael, France, April 2005 (on CD).
7. S. Marburg, H.J. Beer, J. Gier, H.J. Hardtke, R. Rennert and F. Perret, Experimental verification of structural-acoustic modelling and design optimization, *Journal of Sound and Vibration*, 252, 591-615 (2002).
8. I. Hagiwara, D.W. Wang, Q.Z. Shi and R.S. Rao, Reduction of noise inside a cavity by piezoelectric actuators, *Journal of Vibration and Acoustics*, 125, 12-17 (2003).
9. J. Luo and H.C. Gea, Optimal stiffener design for interior sound reduction using a topology optimization based approach, *Journal of Vibration and Acoustics*, 125, 267-273 (2003).
10. C.J. Damaren, Optimal location of collocated piezo-actuator/sensor combinations in spacecraft box structures, *Smart Mater. Struct.*, 12, 494-499 (2003).
11. F.J. Fahy, *Sound and Structural Vibration*, Academic Press, London (1985).